Inorganic Chemistry

Article

pubs.acs.org/IC

Effect of Halogen (Cl, Br) on the Symmetry of Flexible Perovskite-Related Framework

Chunyan Bai,[†,‡] Hongwei Yu,[†,‡] Shujuan Han,*[,†] Shilie Pan,*[,†] Bingbing Zhang,[†,‡] Ying Wang,[†,‡] Hongping Wu,[†] and Zhihua Yang*[,†]

[†]Key Laboratory of Functional Materials and Devices for Special Environments of CAS, Xinjiang Key Laboratory of Electronic Information Materials and Devices, Xinjiang Technical Institute of Physics & Chemistry of CAS, 40-1 South Beijing Road, Urumqi 830011, China

[‡]University of Chinese Academy of Sciences, Beijing 100049, China

Supporting Information

ABSTRACT: The perovskite structure is a good candidate for the design of functional materials. On the basis of the combination of B_6O_{13} groups and XM_6 (X = Cl, Br; M = alkali metals) octahedra, three new perovskite-related crystals $Na_3B_6O_{10}Cl$, $RbNa_2B_6O_{10}Cl$, and $RbNa_2B_6O_{10}Br$ have been synthesized by a high-temperature solution method for the first time. $Na_3B_6O_{10}Cl$ and $RbNa_2B_6O_{10}Cl$ are isostructural and crystallize in the noncentrosymmetric (NCS) space group $P2_12_12_1$ (No. 19), while $RbNa_2B_6O_{10}Br$ belongs to the centrosymmetric (CS) space group *Pnma* (No. 62). The phenomenon that Cl-containing borates are not isostructural with corresponding Br-containing borates is extremely rare among borates. Detailed structure analysis suggests that the difference is owing to the effect of the halogen (Cl, Br) on the symmetry of the flexible perovskite-related framework. In addition, thermal analyses, IR spectroscopy, the UV−vis−NIR diffuse reflectance spectrum, and first-principles theoretical studies have also been performed on the three compounds.

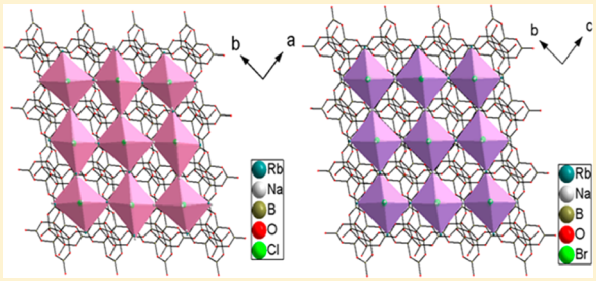

1. INTRODUCTION

Nonlinear optical (NLO) crystals, which are key materials for solid-state lasers to produce coherent light through cascaded frequency conversion, have attracted considerable attention.[1−8] One important prerequisite for a material showing NLO properties is that the crystal must be noncentrosymmetric (NCS). In the last decades, much effort has been made to find out superior performing NCS materials. A number of design strategies include combining second-order Jahn−Teller (SOJT) distortive cations (d^0 transition metals and lone pair cations),[9,10] d^{10} transition metal cations,[11,12] and borates with asymmetric π systems during synthesis.[13,14] However, it is well known that introducing the above cations into borates will make the cutoff edge shift to the red region.

Recently, we realized that crystals with a perovskite-related structure may be ideal candidates for UV NLO materials because the flexible framework of the perovskite-related structure makes them tend to crystallize in NCS space group and have little influence on their cutoff edge. In addition, in our group, by introducing halogen atoms into borate, a series of perovskite-related crystals has been successfully synthesized, such as $K_3B_6O_{10}Cl$,[15] $K_3B_6O_{10}Br$,[16] $Na_3B_6O_{10}Br$.[17] Among these compounds, $K_3B_6O_{10}Cl$ is especially noted, which exhibits a large second-harmonic generation (SHG) response (4 KDP) and deep UV absorption edge (180 nm), and may be a promising UV NLO material. Afterward, based on the relationship between the structure and the properties, four stoichiometric crystals $K_{3-x}Na_xB_6O_{10}Br$ (x = 0.13, 0.67, 1.30, 2.20)[18] have been obtained. In addition, interestingly, the cation plays a profound role to influence the crystal structure and SHG properties. Inspired by the above work, we believe that it is significant to continue an investigation of the $A_3B_6O_{10}X$ (A = alkali metals; X = Cl, Br) system. After extensive efforts, three new perovskite-related crystals $Na_3B_6O_{10}Cl$, $RbNa_2B_6O_{10}Cl$, and $RbNa_2B_6O_{10}Br$ have been discovered by us. Interestingly, although these crystals have similar stoichiometry and exhibit similar perovskite-related structure, they crystallize in different space group. $Na_3B_6O_{10}Cl$ and $RbNa_2B_6O_{10}Cl$ are isostructural and crystallize in the noncentrosymmetric (NCS) space group $P2_12_12_1$ (No. 19), while $RbNa_2B_6O_{10}Br$ belongs to the centrosymmetric (CS) space group *Pnma* (No. 62). To the best of our knowledge, most of the Cl-containing borates are isostructural with corresponding Br-containing borates, such as $Na_{11}B_{21}O_{36}X_2$ (X = Cl, Br),[19] $M_5B_3O_9X$ (M = Ba, Sr; X = Cl, Br),[20] $M_2B_5O_9X$ (M = Pb, Ca, Sr, Ba; X = Cl, Br),[21,22] $Pb_6B_3O_{10}X$ (X = Cl, Br),[23] and so on. However, it is rare that Cl-containing borates are not isostructural with corresponding Br-containing borates, as observed in $Na_3B_6O_{10}Cl$, $RbNa_2B_6O_{10}Cl$, and $RbNa_2B_6O_{10}Br$. More interestingly, there are few reports about the effect of the halogen (Cl, Br) ions on the crystal structure in borates. In this article we discuss the effect of the halogen (Cl, Br) on the

Received: July 26, 2014
Published: September 26, 2014

   dx.doi.org/10.1021/ic501814q | *Inorg. Chem.* 2014, 53, 11213−11220

symmetry of the flexible perovskite-related framework in detail and report the synthesis, structure, thermal behavior, optical properties, as well as band structure calculations of the three compounds.

2. EXPERIMENTAL SECTION

2.1. Reagents. NaCl (Tianjin BaiShi Chemical Reagent Co., 99.0%), NaBr (Tianjin HongYan Chemical Reagent Co., Ltd., 99.0%), Rb_2CO_3 (Xinjiang Chemical Co. Ltd. 99%), Na_2CO_3 (Tianjin HongYan Chemical Co., Ltd., 99.5%), and H_3BO_3 (Tianjin HongYan Chemical Co., Ltd., 99.5%) were used as received.

2.2. Solid-State Synthesis. Polycrystalline powders of $Na_3B_6O_{10}Cl$, $RbNa_2B_6O_{10}Cl$, and $RbNa_2B_6O_{10}Br$ were synthesized via the standard solid-state reaction. Stoichiometric mixtures of Na_2CO_3, NaCl, and H_3BO_3 at a molar ratio 1:1:6 for $Na_3B_6O_{10}Cl$, Rb_2CO_3, Na_2CO_3, NaCl, and H_3BO_3 at a molar ratio 1:1:2:12 for $RbNa_2B_6O_{10}Cl$, and Rb_2CO_3, Na_2CO_3, NaBr, and H_3BO_3 at a molar ratio 1:1:2:12 for $RbNa_2B_6O_{10}Br$ were ground well and packed into Pt crucibles. Raw materials were heated to 500 °C to decompose the carbonate and eliminate the water; then the compounds were gradually heated up to 700 °C for $Na_3B_6O_{10}Cl$ and 650 °C for $RbNa_2B_6O_{10}Cl$ and $RbNa_2B_6O_{10}Br$ and kept at this temperature for 72 h. During the sintering steps the samples were cooled to room temperature and ground. Powders of $Na_3B_6O_{10}Cl$, $RbNa_2B_6O_{10}Cl$, and $RbNa_2B_6O_{10}Br$ were obtained. Powder X-ray diffraction data were carried out with a Bruker D2 PHASER diffractometer equipped with an incident beam monochromator set for Cu Kα radiation (λ = 1.5418 Å). Diffraction patterns were taken from 10° to 70° (2θ) with a scan step width of 0.02° and a fixed counting time of 1 s/step. Diffraction patterns are well agreeable with the calculated ones (Figure S1, Support Information)

2.3. Single-Crystal Growth. Single crystals of $Na_3B_6O_{10}Cl$, $RbNa_2B_6O_{10}Cl$, and $RbNa_2B_6O_{10}Br$ were grown by spontaneous crystallization. A mixture of 0.212 g (2.00 mmol) of Na_2CO_3, 0.818 g (14.00 mmol) of NaCl, and 1.484 g (24.00 mmol) of H_3BO_3 was thoroughly ground for $Na_3B_6O_{10}Cl$. The mixture was then placed in a platinum crucible that was placed into a vertical, programmable temperature furnace. The crucible was gradually heated to 750 °C in air and held for 12 h until the solution became transparent and clear. The homogenized solution was cooled rapidly to 700 °C and then slowly cooled to 550 °C at a rate of 2 °C/h, followed by rapid cooling to room temperature. The other two crystals were obtained through a similar process. In addition, solutions were prepared by melting mixtures of 0.231 g (1.00 mmol) of Rb_2CO_3, 0.106 g (1.00 mmol) of Na_2CO_3, 0.584 g (10.00 mmol) of NaCl, and 1.2366 g (20.00 mmol) of H_3BO_3 for $RbNa_2B_6O_{10}Cl$ and 0.231 g (1.00 mmol) of Rb_2CO_3, 0.106 g (1.00 mmol) of Na_2CO_3, 1.028 g (10.00 mmol) of NaBr, and 1.2366 g (20.00 mmol) of H_3BO_3 for $RbNa_2B_6O_{10}Br$. Crystals were separated mechanically from the crucible for further characterization by single-crystal X-ray measurements.

2.4. Structure Determination. Single crystals of $Na_3B_6O_{10}Cl$, $RbNa_2B_6O_{10}Cl$, and $RbNa_2B_6O_{10}Br$ were selected for structure determination. Their crystal structures were determined by single-crystal X-ray diffraction on an APEX II CCD diffractometer using monochromatic Mo Kα radiation (λ = 0.71073 Å) at 296(2) K and intergrated with the SAINT program.[24] Numerical absorption corrections were carried out using the SCALE program for the area detector. All calculations were performed with programs from the SHELXTL crystallographic software package.[25] The positions of all atoms were refined using full matrix least-squares techniques; final least-squares refinement is on F_0^2 with data having $F_0^2 \geq 2\sigma(F_0^2)$ (F_0, observed structure factors; σ, standard uncertainty). Structures were checked for missing symmetry elements by the program PLATON.[26] For $Na_3B_6O_{10}Cl$, the Flack parameter was refined and converged at 0.43(12), which indicates that the crystal is racemically (inversion) twinned at an approximately 50% ratio, i.e., individual twin domains have dipole moments oriented either "+" or "−".[27] Crystal data and structure refinement information are presented in Table 1. Final refined atomic positions and isotropic thermal parameters are listed in Table S1, Supporting Information. Selected bond distances (in Angstroms) and angles (in degrees) for $Na_3B_6O_{10}Cl$, $RbNa_2B_6O_{10}Cl$, and $RbNa_2B_6O_{10}Br$ are given in Tables S2−S4, Supporting Information.

Table 1. Crystal Data and Structures Refinement for $Na_3B_6O_{10}Cl$, $RbNa_2B_6O_{10}Cl$, and $RbNa_2B_6O_{10}Br$

chemical formula	$Na_3B_6O_{10}Cl$	$RbNa_2B_6O_{10}Cl$	$RbNa_2B_6O_{10}Br$
FW	329.28	391.76	436.22
cryst syst	orthorhombic	orthorhombic	orthorhombic
space group	$P2_12_12_1$	$P2_12_12_1$	$Pnma$
a [Å]	7.437(8)	8.3251(3)	12.769(8)
b [Å]	9.938(11)	9.6543(3)	9.611(6)
c [Å]	12.804(14)	12.7544(4)	8.390(5)
V [Å^3]	946.3(18)	1025.11(6)	1029.6(11)
Z	4	4	4
abs coeff (mm^{-1})	0.588	5.219	8.818
completeness to theta	99.2%	99.8%	99.4%
GOF on F^2	1.059	1.065	1.107
R_1,wR_2[$F_o^2 > 2\sigma(F_o^2)$][a]	R_1 = 0.0386, wR_2 = 0.0917	R_1 = 0.0286, wR_2 = 0.0680	R_1 = 0.0478, wR_2 = 0.1143
R_1, wR_2 (all data)[a]	R_1 = 0.0481, wR_2 = 0.0975	R_1 = 0.0327, wR_2 = 0.0698	R_1 = 0.0778, wR_2 = 0.1282
Flack parameter	0.43(12)	0.072(10)	

[a] $R_1 = \Sigma||F_o| - |F_c||/\Sigma|F_o|$ and $wR_2 = [\Sigma w(F_o^2 - F_c^2)^2/\Sigma wF_o^4]^{1/2}$ for $F_o^2 > 2\sigma(F_o^2)$.

2.5. Powder SHG Measurements. SHG tests were performed on $Na_3B_6O_{10}Cl$ and $RbNa_2B_6O_{10}Cl$ by the Kurtz−Perry method.[28] In general, the SHG efficiency has been shown to depend on particle size, so the compounds were ground and sieved into distinct particle size ranges, 20−38, 38−55, 55−88, 88−105, 105−150, and 150−200 μm. The sample was irradiated with a pulsed infrared beam produced by a Q-switched Nd:YAG laser at a wavelength of 1064 nm. In addition, the microcrystalline KDP served as a reference.

2.6. Infrared Spectroscopy. IR spectra of $Na_3B_6O_{10}Cl$, $RbNa_2B_6O_{10}Cl$, and $RbNa_2B_6O_{10}Br$ were recorded on a Shimadzu IR Affinity-1 Fourier transform infrared spectrometer in the 400−4000 cm^{-1} range. Samples were mixed thoroughly with dried KBr, and characteristic absorption peaks are shown in Figure S2, Supporting Information.

2.7. UV−Vis−NIR Diffuse Reflectance Spectra. Optical diffuse reflectance spectra of $Na_3B_6O_{10}Cl$, $RbNa_2B_6O_{10}Cl$, and $RbNa_2B_6O_{10}Br$ were measured at room temperature with a Shimadzu SolidSpec-3700DUV spectrophotometer. Data were collected in the wavelength range 190−2500 nm. Also, reflectance spectra were converted to absorbance with the Kubelka−Munk function.[29,30]

2.8. Thermal Analysis. The melting behaviors of $Na_3B_6O_{10}Cl$, $RbNa_2B_6O_{10}Cl$, and $RbNa_2B_6O_{10}Br$ were examined on a NETZSCH STA 449C simultaneous analyzer instrument in an atmosphere of flowing N_2. The sample was heated from 25 to 1000 °C at a rate of 10 °C/min.

2.9. Elemental Analysis. Elemental analysis of a single crystal was measured by a VISTA-PRO CCD simultaneous ICP-OES. Crystal samples were dissolved in nitric acid. Elemental analysis results are listed in Table S5, Supporting Information.

2.10. Theoretical Calculations. Electronic structures of the title crystals, including the band structure and full/partial density of states (DOS/PDOS), were performed by a plane-wave pseudopotential package employed in CASTEP.[31] Norm-conserving pseudopotentials (NCP)[32−34] were used. The exchange-correlation functional was a Perdew−Burke−Emzerhoff (PBE) functional within the generalized gradient approximation (GGA).[35] The plane-wave energy cutoff was set at 830.0 eV. The k-point separation for each material was set as 0.035 $Å^{-1}$ in the Brillouin zone. Self-consistent field (SCF) calculations were performed with a convergence criterion of 0.5×10^{-6} eV/atom on the total energy.

dx.doi.org/10.1021/ic501814q | Inorg. Chem. 2014, 53, 11213−11220

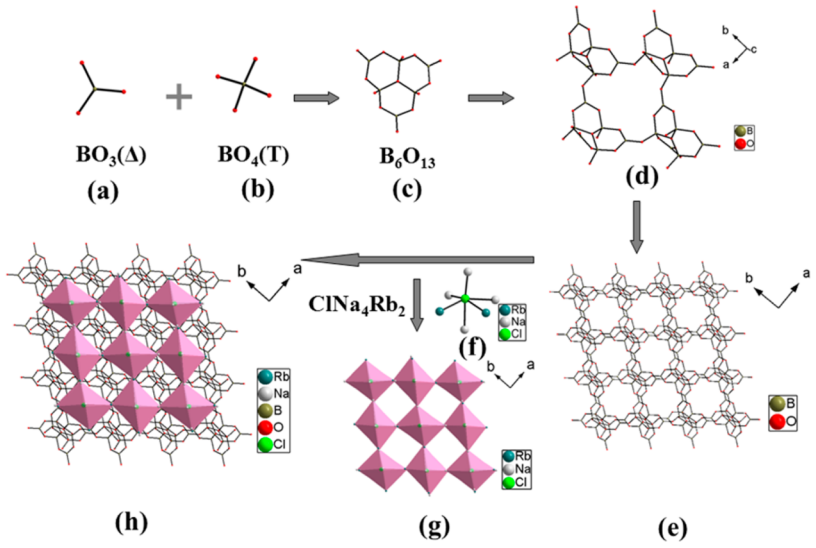

Figure 1. Crystal structure of $RbNa_2B_6O_{10}Cl$: (a) the BO_3 group, (b) the BO_4 group, (c) the B_6O_{13} group, (d) four B_6O_{13} groups, (e) the B_6O_{13} network, (f) the $ClNa_4Rb_2$ octahedron, (g) the $ClNa_4Rb_2$ network, and (h) the crystal structure of $RbNa_2B_6O_{10}Cl$. $ClNa_4Rb_2$ octahedra are shown in rose.

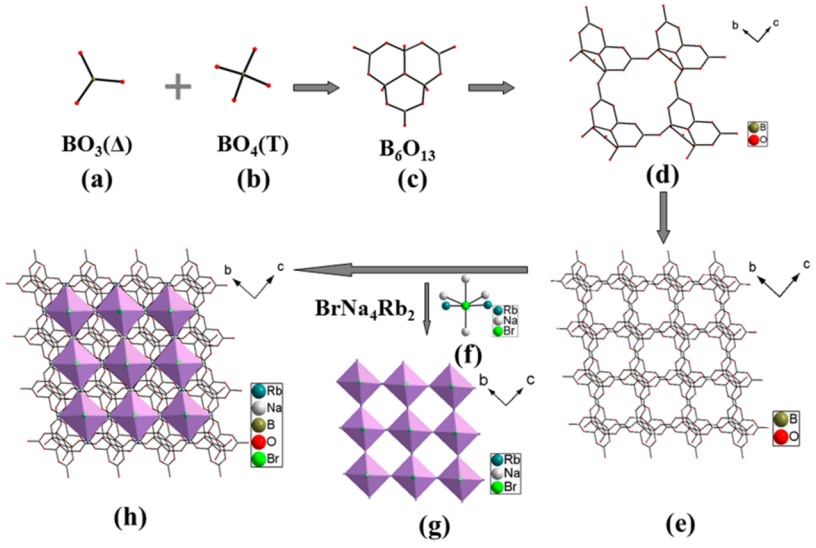

Figure 2. Crystal structure of $RbNa_2B_6O_{10}Br$: (a) the BO_3 group, (b) the BO_4 group, (c) the B_6O_{13} group, (d) four B_6O_{13} groups, (e) the B_6O_{13} network, (f) the $BrNa_4Rb_2$ octahedron, (g) the $BrNa_4Rb_2$ network, and (h) the crystal structure of $RbNa_2B_6O_{10}Br$. $BrNa_4Rb_2$ octahedra are shown in lavender.

3. RESULTS AND DISCUSSION

3.1. Crystal Structure. All three crystals of $Na_3B_6O_{10}Cl$, $RbNa_2B_6O_{10}Cl$, and $RbNa_2B_6O_{10}Br$ exhibit an intricate 3D network, which are built up by B_6O_{13} groups and six-coordinated XM_6 (X = Cl, Br; M = Na, Rb) polyhedra. The individual XM_6 (X = Cl, Br; M = Na, Rb) octahedra are linked together through vertices to create a distorted perovskite-related framework. By analogy with the mineral perovskite $CaTiO_3$, the positions of large calcium cations are occupied by the B_6O_{13} groups, the positions of titanium atoms are similar to those of halogen atoms, and the positions of oxygen atoms are similar to the positions of alkali metals. Hence, their formulas can be represented as $CaTiO_3$ and $[B_6O_{10}]XM_3$ (X = Cl, Br; M = Rb, Na) (Figure S3, Supporting Information).[15a] However, they crystallize in various space groups: $Na_3B_6O_{10}Cl$ and $RbNa_2B_6O_{10}Cl$ are isostructural and crystallize in NCS orthorhombic symmetry with space group $P2_12_12_1$, while $RbNa_2B_6O_{10}Br$ belongs to another space group *Pnma* of the orthorhombic system. Structures are described in detail as follows.

3.1.1. Structures of $Na_3B_6O_{10}Cl$ and $RbNa_2B_6O_{10}Cl$. $Na_3B_6O_{10}Cl$ and $RbNa_2B_6O_{10}Cl$ are isostructural and have a similar 3D framework, except that one type of Na atom is replaced by the Rb atom. Hence, only the structure of $RbNa_2B_6O_{10}Cl$ will be discussed in detail as a representation. In the asymmetric unit of $RbNa_2B_6O_{10}Cl$ there are one unique Rb atom, two unique Na atoms, six unique B atoms, ten unique O atoms, and one unique Cl atom (Table S1, Supporting Information). The 3D framework is composed of B_6O_{13} groups and $ClNa_4Rb_2$ octahedra (Figure 1). The B_6O_{13} (Figure 1c) group is formed by three BO_4 tetrahedra (T) shared by the oxygen vertex and three BO_3 triangles (Δ) attached to the terminal vertices of these tetrahedra, which can be represented as $6[3\Delta + 3T]$ according to the definition given by Burns et al.[36] The B_6O_{13} groups link with each other by oxygen sharing to form a 3D network with tunnels pointing along the *c* axis (Figure 1e). The B_6O_{13} groups align along the *b* axis almost reversely in the *bc*

dx.doi.org/10.1021/ic501814q | *Inorg. Chem.* 2014, 53, 11213−11220

plane (Figure S4.1, Supporting Information). $ClNa_4Rb_2$ octahedra are linked together through vertices to create a distorted perovskite-related framework (Figure 1g). The B_6O_{13} and $ClNa_4Rb_2$ networks are interweaved to forming an intricate 3D network (Figure 1h).

The Na1 atoms are coordinated by six O atoms and two Cl atoms to form a distorted $Na1O_6Cl_2$ polyhedron. The Na2 and Rb1 atoms are coordinated by four O atoms and two Cl atoms (Figure S5b, Supporting Information). The bond valence sums of each atom in $Na_3B_6O_{10}Cl$ and $RbNa_2B_6O_{10}Cl$ were calculated and are listed in Table S1, Supporting Information. These valence sums agree with expected oxidation states.

3.1.2. Structures of $RbNa_2B_6O_{10}Br$. $RbNa_2B_6O_{10}Br$ is isostructural with the previously reported $Na_3B_6O_{10}Br$.[17] The difference between the two crystal structures is that one type of Na atom which is located in the 4b site of the Wyckoff position is replaced by the Rb atom. In the asymmetric unit of $RbNa_2B_6O_{10}Br$ there are one unique Rb atom, two unique Na atoms, four unique B atoms, six unique O atoms, and one unique Br atom (Table S1, Supporting Information). Similar to that of $RbNa_2B_6O_{10}Cl$, the structure of $RbNa_2B_6O_{10}Br$ can also be described as the B_6O_{13} network and $BrNa_4Rb_2$ network interweaved to form an intricate 3D network (Figure 2). The B_6O_{13} groups align along the *b* axis totally reversely in the *ab* plane (Figure S4.2, Supporting Information). The Br atoms are located in the six coordination environment bonding to two Na1 atoms, two Na2 atoms, and two Rb2 atoms (Figure 2f). The Na1 atoms are coordinated by six O atoms and two Br atoms to form a distorted $Na1O_6Br_2$ polyhedron. The Na2 and Rb1 atoms are coordinated by four O atoms and two Br atoms (Figure S5c, Supporting Information). The Na−Br bond distances range from 3.09(4) to 3.33(2) Å, the Na(1)−Br(1)−Na(1) bond angle is 176.50(1)°, and the Rb(1)−Br(1)−Na(2) bond angles are both 155.82(1)°. Compared to $RbNa_2B_6O_{10}Br$, the Na−Cl bond distances lie in a large interval 2.77(7)−4.14(1) Å for $Na_3B_6O_{10}Cl$ and 2.77(2)−3.43(4) Å for $RbNa_2B_6O_{10}Cl$. The Na(3)−Cl(1)−Na(3) bond angle is 164.89(5)° and Na(1)−Cl(1)−Na(2) bond angles are 154.98(6)° and 161.86(3)° for $Na_3B_6O_{10}Cl$. The Na(1)−Cl(1)−Na(1) bond angle is 179.69(6)° and Rb(1)−Cl(1)−Na(2) bond angles are 152.98(4)° and 157.01(5)° for $RbNa_2B_6O_{10}Cl$ (Table 3). The bond valence sums of each atom in $RbNa_2B_6O_{10}Br$ were calculated and are listed in Table S1, Supporting Information. These valence sums agree with expected oxidation states.

3.2. Effect of Halogen (Cl, Br) on the Symmetry of Flexible Perovskite-Related Framework. Although the three crystals reported in this paper and $Na_3B_6O_{10}Br$[17] reported previously possess a similar stoichiometric ratio and all exhibit a perovskite-related structure, out-of-center distortions of XM_6 (X = Cl, Br) octahedra controlled by the size and coordination environment of the X atoms make them crystallize in different space groups. By analogy with the mineral perovskite ABX_3, the positions of A cations are occupied by the B_6O_{13} groups, the positions of B atoms are similar to those of halogen atoms, and the positions of X atoms are similar to the positions of alkali metals.[15] As is known to all, the tilting of the anion octahedra, displacements of the cations, and distortions of the octahedra in ABX_3 make the perovskite structures abundant.[37,38] Herein, the structure of $A_3B_6O_{10}X$ may be changed if the XM_6 octahedra are tilted or distorted.

Following the criteria proposed by Halasyamani,[39] all of the distortions of XM_6 octahedra in the four crystals distort along the C3 [111] direction and the magnitudes of out-of-center distortions can be calculated. Octahedron distortion, Δd parameter, is defined as

$$\Delta d = \frac{|(M-O1)-(M-O4)|}{|\cos\theta_1|} + \frac{|(M-O2)-(M-O5)|}{|\cos\theta_2|} + \frac{|(M-O3)-(M-O6)|}{|\cos\theta_3|}$$

where the pairs (O1, O4), (O2, O5), and (O3, O6) are the atoms that constitute the octahedron and are located in opposite positions from each other.[39,40] The obtained Δd values for the four XM_6 octahedra in $Na_3B_6O_{10}Cl$, $RbNa_2B_6O_{10}Cl$, $Na_3B_6O_{10}Br$, and $RbNa_2B_6O_{10}Br$ are 2.342, 1.597, 0.933, and 0.502, respectively, which can be seen in Table 2. It is of interest to note that the magnitudes of out-of-center distortion of ClM_6 octahedra are larger than those of BrM_6 octahedra as a result of the two weak Na−Cl bonds in ClM_6 octahedra (Table 3, Figure 3). In the four crystals, the different distortions of the XM_6 octahedron make the connecting angles between XM_6 octahedra different, which further influences the overall symmetry of the perovskite-related framework of the crystal.

Table 2. Direction and Magnitude (Δd) of the out-of-Center Distortion of the XM_6 Octahedra in $K_3B_6O_{10}X$, $Na_3B_6O_{10}X$, and $RbNa_2B_6O_{10}X$ (X = Cl, Br)

compd	space group	species	direction	Δd
$K_3B_6O_{10}Cl$	*R*3*m*	ClK_6	C3[111]	0.137
$K_3B_6O_{10}Br$	*R*3*m*	BrK_6	C3[111]	0.027
$Na_3B_6O_{10}Cl$	$P2_12_12_1$	$ClNa_6$	C3[111]	2.342
$Na_3B_6O_{10}Br$	*Pnma*	$BrNa_6$	C3[111]	0.933
$RbNa_2B_6O_{10}Cl$	$P2_12_12_1$	$ClNa_4Rb_2$	C3[111]	1.597
$RbNa_2B_6O_{10}Br$	*Pnma*	$BrNa_4Rb_2$	C3[111]	0.502

According to the reference,[38] when the cations are displaced or the octahedra are distorted (or tilted), different types of structures are produced, which are always of lower symmetry. Since the magnitudes of the out-of-center distortion of BrM_6 octahedra are smaller than those of ClM_6 octahedra, the symmetry is decreased from Br-containing borates (*Pnma*) to Cl-containing borate ($P2_12_12_1$) in the four crystals. With the transition from the space group *Pnma* to $P2_12_12_1$, the glide planes *n* and *a* and the mirror plane *m* are lost. A detailed structure comparison referred to $RbNa_2B_6O_{10}Cl$ and $RbNa_2B_6O_{10}Cl$ was carried out. As shown in Figure S6.1, Supporting Information, looking down the *b* axis of $RbNa_2B_6O_{10}Br$, the $BrNa_4Rb_2$ building unit generates itself by the *n*-glide plane. Looking down the *a* axis of $RbNa_2B_6O_{10}Br$ (Figure S6.2, Supporting Information), the $BrNa_4Rb_2$ building unit operates itself by the *m*-mirror plane. Seen from the *c* axis (Figure S6.3, Supporting Information), the $BrNa_4Rb_2$ octahedron operates itself by the *a*-glide plane and eventually crystallizes in the *Pnma* symmetry. Differently, the (100), (010), (001) view of $RbNa_2B_6O_{10}Cl$ reveals that the $ClNa_4Rb_2$ octahedra are related only by 2_1-screw axes, and $RbNa_2B_6O_{10}Cl$ eventually crystallizes in the $P2_12_12_1$ symmetry.

Different from the above four crystals, $K_3B_6O_{10}Cl$[15] and $K_3B_6O_{10}Br$[16] are isostructural, which can be explained from XK_6 octahedra distortion. As can be seen from Table 2, the obtained Δd values for XK_6 octahedra in $K_3B_6O_{10}Cl$ and $K_3B_6O_{10}Br$ are

dx.doi.org/10.1021/ic501814q | Inorg. Chem. 2014, 53, 11213−11220

Table 3. Bond Lengths (Angstroms) and Selected Angles (degrees) within the XM_6 Octahedra in $Na_3B_6O_{10}X$, $K_3B_6O_{10}X$, and $RbNa_2B_6O_{10}X$ (X = Cl, Br)

	$Na_3B_6O_{10}Cl$		
Na(1)−Cl(1)	2.77(7)	Na(1)−Cl(1)	4.14(1)
Na(2)−Cl(1)	2.89(2)	Na(2)−Cl(1)	2.82(6)
Na(3)−Cl(1)	2.87(9)	Na(3)−Cl(1)	3.82(1)
Na(1)−Cl(1)−Na(2)	161.86(3)	Na(3)−Cl(1)−Na(3)	164.89(5)
Na(1)−Cl(1)−Na(2)	154.98(6)		
	$Na_3B_6O_{10}Br$		
Na(1)−Br(1)	3.39(8)	Na(1)−Br(1)	3.19(9)
Na(2)−Br(1)	3.33(9)	Na(2)−Br(1)	3.33(9)
Na(3)−Br(1)	3.00(1)	Na(3)−Br(1)	3.00(1)
Na(1)−Br(1)−Na(1)	170.59(6)	Na(2)−Br(1)−Na(3)	157.85(1)
Na(2)−Br(1)−Na(3)	157.85(1)		
	$K_3B_6O_{10}Cl$		
K(1)−Cl(1)	3.31(1)	K(1)−Cl(1)	3.31(1)
K(1)−Cl(1)	3.31(1)	K(1)−Cl(1)	3.26(6)
K(1)−Cl(1)	3.26(6)	K(1)−Cl(1)	3.26(6)
K(1)−Cl(1)−K(1)	164.19(6)	K(1)−Cl(1)−K(1)	164.19(6)
K(1)−Cl(1)−K(1)	164.19(6)		
	$K_3B_6O_{10}Br$		
K(1)−Br(1)	3.32(1)	K(1)−Br(1)	3.32(1)
K(1)−Br(1)	3.32(1)	K(1)−Br(1)	3.31(2)
K(1)−Br(1)	3.31(2)	K(1)−Br(1)	3.31(1)
K(1)−Br(1)−K(1)	161.38(2)	K(1)−Br(1)−K(1)	161.38(2)
K(1)−Br(1)−K(1)	161.40(2)		
	$RbNa_2B_6O_{10}Cl$		
Na(1)−Cl(1)	2.96 (2)	Na(2)−Cl(1)	3.84(1)
Na(1)−Cl(1)	3.43(4)	Rb(1)−Cl(1)	3.20(1)
Na(2)−Cl(1)	2.77(2)	Rb(1)−Cl(1)	3.26(1)
Rb(1)−Cl(1)−Na(2)	152.98(4)	Rb(1)−Cl(1)−Na(2)	157.01(5)
Na(1)−Cl(1)−Na(1)	179.69(6)		
	$RbNa_2B_6O_{10}Br$		
Na(1)−Br(1)	3.09(4)	Na(2)−Br(1)	3.20(2)
Na(1)−Br(1)	3.30(5)	Rb(1)−Br(1)	3.33(2)
Na(2)−Br(1)	3.20(2)	Rb(1)−Br(1)	3.33(2)
Rb(1)−Br(1)−Na(2)	155.82(1)	Rb(1)−Br(1)−Na(2)	155.82(1)
Na(1)−Br(1)−Na(1)	176.50(1)		

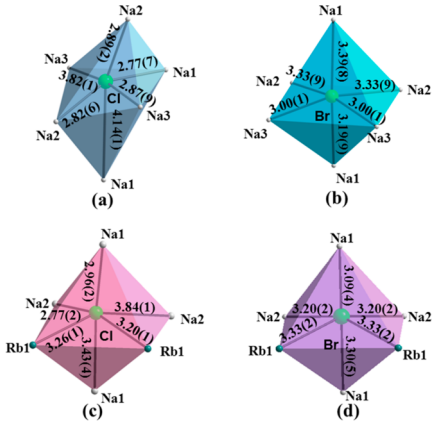

Figure 3. Comparison of XM_6 octahedron: (a) $ClNa_6$, (b) $BrNa_6$, (c) $ClNa_4Rb_2$, and (d) $BrNa_4Rb_2$. $ClNa_6$ octahedron is shown in pale blue, $BrNa_6$ octahedron is shown in sky blue, $ClNa_4Rb_2$ octahedron is shown in rose, and $BrNa_4Rb_2$ octahedron is shown in lavender.

0.137 and 0.027, which fall into the second and first category defined by Halasyamani,[39] respectively. In addition, these values correspond to weak and no distortion, respectively. The distortions of XM_6 octahedra in $K_3B_6O_{10}Cl$ and $K_3B_6O_{10}Br$ are too small to make their structure vary.

3.3. SHG Properties. SHG measurements on polycrystalline samples of $Na_3B_6O_{10}Cl$ and $RbNa_2B_6O_{10}Cl$ reveal that both of them exhibit no observable green light in our experimental condition. The SHG coefficients were also calculated from the band wave functions using the length-gauge formalism derived by Aversa and Sipe at a zero frequency limit.[41] Calculated SHG coefficients of $Na_3B_6O_{10}Cl$ and $RbNa_2B_6O_{10}Cl$ are $d_{14} = -0.06$ and 0.03 pm/V, respectively. Since the SHG coefficient is so small we cannot see the SHG effect in the SHG experiment.

3.4. Infrared Spectrum. Figure S2, Supporting Information, presents the infrared spectra of $Na_3B_6O_{10}Cl$, $RbNa_2B_6O_{10}Cl$, and $RbNa_2B_6O_{10}Br$, and they are similar. The assignments of infrared spectra of the three compounds are listed in Table S6, Supporting Information. Referring to the literatures,[42] the peaks at 1347−1187 and 963−908 cm^{-1} can be assigned to the asymmetric stretching and symmetric stretching vibrations of BO_3, respectively. Peaks located at 1083−1012 and 860−797 cm^{-1} arise from the asymmetric stretching and symmetric stretching vibrations of BO_4, respectively. Peaks observed in the region of 733−641 cm^{-1} are attributed to the out-of-bending of BO_3. Peaks below 600 cm^{-1} characterize the bending of BO_3 and BO_4. Infrared spectra further confirm the existence of BO_3 triangles and BO_4 tetrahedra, which is consistent with the results obtained from single-crystal X-ray structural analyses.

3.5. UV−Vis−NIR Diffuse Reflectance Spectroscopy. UV−vis−NIR diffuse reflectance spectra of $Na_3B_6O_{10}Cl$, $RbNa_2B_6O_{10}Cl$, and $RbNa_2B_6O_{10}Br$ in the region 190−2500 nm are shown in Figure S7, Supporting Information. It is clear that the three compounds have no obvious absorption from 320 to 2500 nm, but the absorption sharply increases below 320 nm, and the cutoff edges for the three compounds are below 190 nm.

3.6. Thermal Analysis. DSC/TG curves of the three crystals are shown in Figure 4. It can be seen that there is one endothermic peak at 757, 692, and 709 °C on the DSC curves for $Na_3B_6O_{10}Cl$, $RbNa_2B_6O_{10}Cl$, and $RbNa_2B_6O_{10}Br$, respectively, along with weight loss on the TG curves. Analysis of the powder XRD pattern of the solidified melt reveals that the entire solid product exhibits a diffraction pattern different from that of the initial pure powder for $Na_3B_6O_{10}Cl$, as shown in Figure S8a, Supporting Information. It demonstrates that $Na_3B_6O_{10}Cl$ is an incongruently melting compound. Analysis of the powder XRD pattern of the $RbNa_2B_6O_{10}Cl$ and $RbNa_2B_6O_{10}Br$ solidified melt reveals that the main phases are $RbNa_2B_6O_{10}Cl$ and $RbNa_2B_6O_{10}Br$, respectively (Figures S8b and S8c, Supporting Information), and there are some extra peaks, which may come from decomposition and volatilization of the samples. Analysis of the powder XRD pattern of the long-term quenching reveals that the entire solid product exhibits a diffraction pattern different from that of the initial pure powder for $RbNa_2B_6O_{10}Br$, as shown in Figure S8c, Supporting Information. Analysis of the powder XRD pattern of the long-term annealing reveals that the entire solid product exhibits a diffraction pattern different from that of the initial pure powder for $RbNa_2B_6O_{10}Cl$, as shown in Figure S8b, Supporting Information. It demonstrates that $RbNa_2B_6O_{10}Cl$ and $RbNa_2B_6O_{10}Br$ are incongruently melting compounds.

3.7. Theoretical Calculations. The electronic band structures of $Na_3B_6O_{10}Cl$, $RbNa_2B_6O_{10}Cl$, and $RbNa_2B_6O_{10}Br$ calculated by the GGA method are plotted along high-symmetry *k* points in Figure S9, Supporting Information. All three crystals are direct band-gap materials with calculated band gaps of 5.17

dx.doi.org/10.1021/ic501814q | Inorg. Chem. 2014, 53, 11213−11220

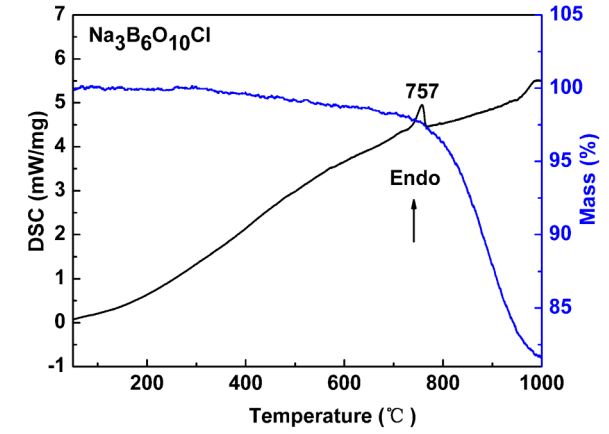

(a) $Na_3B_6O_{10}Cl$

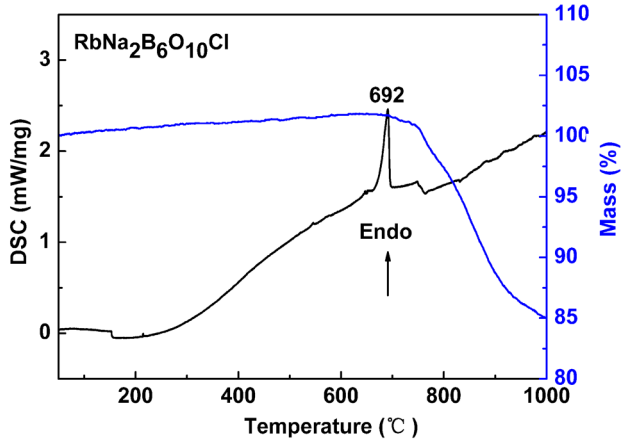

(b) $RbNa_2B_6O_{10}Cl$

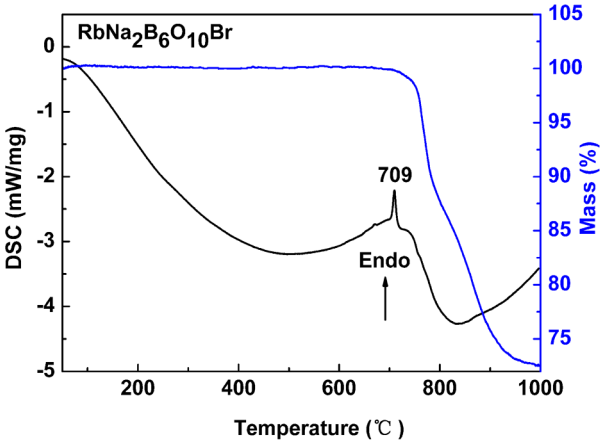

(c) $RbNa_2B_6O_{10}Br$

Figure 4. TG/DSC curves for (a) $Na_3B_6O_{10}Cl$, (b) $RbNa_2B_6O_{10}Cl$, and (c) $RbNa_2B_6O_{10}Br$.

($Na_3B_6O_{10}Cl$), 5.06 ($RbNa_2B_6O_{10}Cl$), and 5.07 eV ($RbNa_2B_6O_{10}Br$), which are relatively smaller than the experimental optical gaps (>6.5 eV) due to a typical disadvantage in density functional theory (DFT) calculations. The PDOS of $Na_3B_6O_{10}Cl$ is displayed in Figure 5. It is clear that the nonbonding Cl 3p and O 2p orbitals are located at the top of the

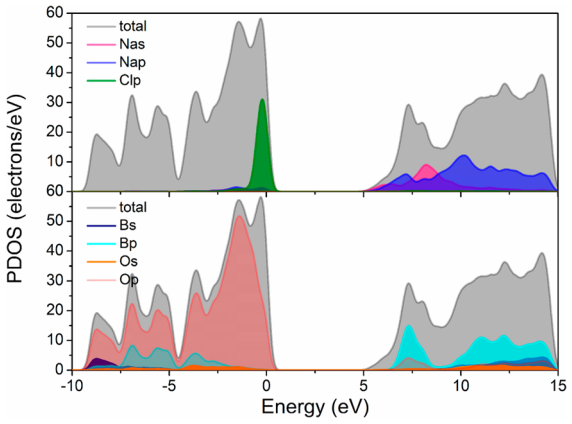

Figure 5. Full density of states (DOS) and partial density of states (PDOS) of $Na_3B_6O_{10}Cl$.

valence band. The obvious mixture of O 2p and B 2p at an energy range from −10 to 3 eV illustrates the B−O convalent bond. The bottom of the conduction band is occupied by Na s p, B 2p, and O 2p orbitals. The PDOSs of the other two crystals (see Figure S10, Supporting Information) are similar to that of $Na_3B_6O_{10}Cl$ due to all three crystals having similar building units and chemical environment.

4. CONCLUSIONS

This study is a continuation of a systematic investigation of the $A_3B_6O_{10}X$ (A = alkali metals; X = Cl, Br) system. In this system, the rare example that Cl-containing borates ($Na_3B_6O_{10}Cl$, $RbNa_2B_6O_{10}Cl$) are not isostructural with corresponding Br-containing borates ($Na_3B_6O_{10}Br$, $RbNa_2B_6O_{10}Br$) has been reported. Close structural examination suggests that out-of-center distortion of XM_6 (X = Cl, Br) octahedra controlled by the size and coordination environment of the X atoms makes them crystallize in various perovskite-related frameworks. Diffuse-reflectance spectra exhibit that all of the three compounds have a wide transparency range from the UV to the IR region, which indicates that they are potentially an optical material in the deep-UV region. In the future, research on the $A_3B_6O_{10}X$ (A = alkali metals; X = Cl, Br) system will be further expanded.

■ ASSOCIATED CONTENT

Supporting Information

X-ray data in CIF format; tables of atomic coordinates, equivalent isotropic displacement parameters and bond valences, selected bond lengths and angles, elemental analysis, assignment of infrared spectra; figures of powder X-ray diffraction, infrared spectra, perovskite structure of $CaTiO_3$ and $RbNa_2B_6O_{10}Br$, boron−oxygen framework of $RbNa_2B_6O_{10}Cl$ and $RbNa_2B_6O_{10}Br$, coordination environment of the cation, comparison of $ClNa_4Rb_2$ and $BrNa_4Rb_2$ networks in $RbNa_2B_6O_{10}Cl$ and $RbNa_2B_6O_{10}Br$, UV−vis−NIR diffuse-reflectance spectra, powder XRD patterns before and after melting, long-term quenching and annealing, calculated band structures, full density of states (DOS), and partial density of states (PDOS). This material is available free of charge via the Internet at http://pubs.acs.org.

■ AUTHOR INFORMATION

Corresponding Authors

*E-mail: hansj@ms.xjb.ac.cn.
*E-mail: slpan@ms.xjb.ac.cn.

*E-mail: zhyang@ms.xjb.ac.cn.

Notes

The authors declare no competing financial interest.

■ ACKNOWLEDGMENTS

This work was supported by the National Natural Science Foundation of China (Grant Nos. 51302307, 51172277, U1129301, U1303392), Western Light of Chinese Academy of Sciences (Grant No. XBBS201220, XBBS201214), High-level Professional and Technical Personnel of Autonomous region, Xinjiang International Science & Technology Cooperation Program (20146001), National Key Basic Research Program of China (Grant No. 2012CB626803), and. Main Direction Program of Knowledge Innovation of Chinese Academy of Sciences (Grant No. KJCX2-EW-H03-03).

■ REFERENCES

(1) (a) Chen, C. T.; Wu, B. C.; Jiang, A. D.; You, G. M. *Sci. Sin., Ser. B (Engl. Ed.)* **1985**, *28*, 235−243. (b) Chen, C. T.; Wu, Y. C.; Jiang, A. D.; Wu, B. C.; You, G. M.; Li, R. K.; Lin, S. J. *J. Opt. Soc. Am. B* **1989**, *6*, 616−621.

(2) (a) Becker, P. *Adv. Mater.* **1998**, *10*, 979−992. (b) Becker, P.; Frohlich, R. Z. *Z. Naturforsch. B* **2004**, *59*, 256−258.

(3) (a) Huang, H. W.; Yao, J. Y.; Lin, Z. S.; Wang, X. Y.; He, R.; Yao, W. J.; Zhai, N. X.; Chen, C. T. *Angew. Chem., Int. Ed.* **2011**, *123*, 9307−9310. (b) Ok, K. M.; Chi, E. O.; Halasyamani, P. S. *Chem. Soc. Rev.* **2006**, *35*, 710−717.

(4) (a) Yu, H. W.; Pan, S. L.; Wu, H. P.; Zhao, W. W.; Zhang, F. F.; Li, H. Y.; Yang, Z. H. *J. Mater. Chem.* **2012**, *22*, 2105−2110. (b) Pan, S. L.; Wu, Y. C.; Fu, P. Z.; Zhang, G. C.; Li, Z. H.; Du, C. X.; Chen, C. T. *Chem. Mater.* **2003**, *15*, 2218−2221. (c) Yang, Y.; Pan, S. L.; Li, H. Y.; Han, J.; Chen, Z. H.; Zhao, W. W.; Zhou, Z. X. *Inorg. Chem.* **2011**, *50*, 2415−2419. (d) Yang, Y.; Pan, S. L.; Hou, X. L.; Wang, C. Y.; Poeppelmeier, K. R.; Chen, Z. H.; Wu, H. P.; Zhou, Z. X. *J. Mater. Chem.* **2011**, *21*, 2890−2894.

(5) (a) Wang, L.; Pan, S. L.; Chang, L. X.; Hu, J. Y.; Yu, H. W. *Inorg. Chem.* **2012**, *51*, 1852−1858. (b) Wang, S. C.; Ye, N.; Li, W.; Zhao, D. *J. Am. Chem. Soc.* **2010**, *132*, 8779−8786. (c) Wang, S. C.; Ye, N. *J. Am. Chem. Soc.* **2011**, *133*, 11458−11461. (d) Pan, S. L.; Smit, J. P.; Watkins, B.; Marvel, M. R.; Stern, C. L.; Poeppelmeier, K. R. *J. Am. Chem. Soc.* **2006**, *128*, 11631−11634.

(6) (a) Mao, J. G.; Jiang, H. L.; Fang, K. *Inorg. Chem.* **2008**, *47*, 8498−8510. (b) Yao, W. J.; Huang, H. W.; Yao, J. Y.; Xu, T.; Jiang, X. X.; Lin, Z. S.; Chen, C. T. *Inorg. Chem.* **2013**, *52*, 6136−6141. (c) Maggard, P. A.; Stern, C. L.; Poepplemeier, K. R. *J. Am. Chem. Soc.* **2001**, *123*, 7742−7743. (d) Kong, F.; Huang, S. P.; Sun, Z. M.; Mao, J. G.; Cheng, W. D. *J. Am. Chem. Soc.* **2006**, *128*, 7750−7751.

(7) (a) Sasaki, T.; Mori, Y.; Yoshiura, M.; Yap, Y. K.; Kamimura, T. *Mater. Sci. Eng., R* **2000**, *30*, 1−54. (b) Keszler, D. A. *Curr. Opin. Solid State Mater. Sci.* **1996**, *1*, 204−211.

(8) (a) Rong, C.; Yu, Z.; Wang, Q.; Zheng, S. T.; Pan, C. Y.; Deng, F.; Yang, G. Y. *Inorg. Chem.* **2009**, *48*, 3650−3659. (b) Hu, Z. G.; Yoshimura, M.; Muramatsu, K.; Mori, Y.; Sasaki, T. J. *Appl. Phys.* **2002**, *41*, 1131−1133. (c) Chen, G. J.; Wu, Y. C.; Fu, P. Z. *J. Cryst. Growth* **2006**, *292*, 449−453.

(9) (a) Ra, H. S.; Ok, K. M.; Halasyamani, P. S. *J. Am. Chem. Soc.* **2003**, *125*, 7764−7765. (b) Sykora, R. E.; Ok, K. M.; Halasyamani, P. S.; Albrecht-Schmitt, T. E. *J. Am. Chem. Soc.* **2002**, *124*, 1951−1957. (c) Huang, Y. Z.; Wu, L. M.; Wu, X. T.; Li, L. H.; Chen, L.; Zhang, Y. F. *J. Am. Chem. Soc.* **2010**, *132*, 12788−12789. (d) Chi, E. O.; Ok, K. M.; Porter, Y.; Halasyamani, P. S. *Chem. Mater.* **2006**, *18* (8), 2070−2074. (e) Porter, Y.; Ok, K. M.; Bhuvanesh, N. S. P.; Halasyamani, P. S. *Chem. Mater.* **2001**, *13* (5), 1910−1915.

(10) (a) Halasyamani, P. S.; Poeppelmeier, K. R. *Chem. Mater.* **1998**, *10*, 2753−2769. (b) Zhao, S. G.; Jiang, X. X.; He, R.; Zhang, S. Q.; Sun, Z. H.; Luo, J. H.; Lin, Z. S.; Hong, M. C. *J. Mater. Chem. C* **2013**, *1*, 2906−2912. (c) Phanon, D.; Gautier-Luneau, I. *Angew. Chem., Int. Ed.* **2007**, *46*, 8488−8491. (d) Jo, H.; Kim, Y. H.; Lee, D. W.; Ok, K. M. *Dalton Trans.* **2014**, *43*, 11752−11758. (e) Donakowski, M. D.; Gautier, R.; Yeon, J.; Moore, D. T.; Nino, J. C.; Halasyamani, P. S.; Poeppelmeier, K. R. *J. Am. Chem. Soc.* **2012**, *134* (18), 7679−7689.

(11) (a) Zhang, J. H.; Hu, C. L.; Xu, X.; Kong, F.; Mao, J. G. *Inorg. Chem.* **2011**, *50*, 1973−1982. (b) Yang, B. P.; Hu, C. L.; Xu, X.; Huang, C.; Mao, J. G. *Inorg. Chem.* **2013**, *52*, 5378−5384. (c) Lee, D. W.; Ok, K. M. *Inorg. Chem.* **2013**, *52*, 5176−5184. (d) Sorensen, E. M.; Izumi, H. K.; Vaughey, J. T.; Stern, C. L.; Poeppelmeier, K. R. *J. Am. Chem. Soc.* **2005**, *127* (17), 6347−6352. (e) Xu, X.; Yang, B. P.; Huang, C.; Mao, J. G. *Inorg. Chem.* **2014**, *53* (3), 1756−1763.

(12) (a) Zhao, S. G.; Zhang, J.; Zhang, S. Q.; Sun, Z. H.; Lin, Z. S.; Wu, Y. C.; Hong, M. C.; Luo, J. H. *Inorg. Chem.* **2014**, *53*, 2521−2527. (b) Lee, D. W.; Kim, S. B.; Ok, K. M. *Dalton Trans.* **2012**, *41*, 8348−8353. (c) Kim, Y. H.; Lee, D. W.; Ok, K. M. *Inorg. Chem.* **2014**, *53*, 1250−1256. (d) Lee, D. W.; Oh, S. J.; Halasyamani, P. S.; Ok, K. M. *Inorg. Chem.* **2011**, *50*, 4473−4480.

(13) (a) Wu, Y. C.; Sasaki, T.; Nakai, S.; Yokotani, A.; Tang, H. G.; Chen, C. T. *Appl. Phys. Lett.* **1993**, *62*, 2614−2615. (b) Chen, C. T.; Ye, N.; Lin, J.; Jiang, J.; Zeng, W. R.; Wu, B. C. *Adv. Mater.* **1999**, *11*, 1071−1078. (c) Inaguma, Y.; Yoshida, M.; Katsumata, T. *J. Am. Chem. Soc.* **2008**, *130*, 6704−6705.

(14) (a) Jiang, H.; Kong, F.; Fan, Y.; Mao, J. G. *Inorg. Chem.* **2008**, *47*, 7430−7437. (b) Zhang, D.; Johnsson, M. *Acta Crystallogr.* **2008**, *E64*, i26/1. (c) Yu, H. W.; Wu, H. P.; Pan, S. L.; Yang, Z. H.; Su, X.; Zhang, F. F. *J. Mater. Chem.* **2012**, *22*, 9665−9670.

(15) (a) Wu, H. P.; Pan, S. L.; Poeppelmeier, K. R.; Li, H. Y.; Jia, D. Z.; Chen, Z. H.; Fan, X. Y.; Yang, Y.; Rondinelli, J. M.; Luo, H. S. *J. Am. Chem. Soc.* **2011**, *133*, 7786−7790. (b) Wu, H. P.; Pan, S. L.; Yu, H. W.; Jia, D. Z.; Chang, A. M.; Li, H. Y.; Huang, X. *CrystEngComm* **2012**, *14* (3), 799−803.

(16) (a) Zhang, M.; Pan, S. L.; Fan, X. Y.; Zhou, Z. X.; Poeppelmeier, K. R.; Yang, Y. *CrystEngComm* **2011**, *13*, 2899−2903. (b) Fan, X. Y.; Zhang, M.; Pan, S. L.; Yang, Y.; Zhao, W. W. *Mater. Lett.* **2012**, *68*, 374−377. (c) Zhang, M.; Su, X.; Pan, S. L.; Wang, Z.; Zhang, H.; Yang, Z. H.; Zhang, B. B.; Dong, L. Y.; Wang, Y.; Zhang, F. F.; Yang, Y. *J. Phys. Chem. C* **2014**, *118*, 11849−11856. (d) Al-Ama, A. G.; Belokoneva, E. L.; Stefanovich, S. Yu.; Dimitrova, O. V.; Mochenova, N. N. *Kristallografiya* **2006**, *51*, 225−230.

(17) Chen, Z. H.; Pan, S. L.; Dong, X. Y.; Yang, Z. H.; Zhang, M.; Su, X. *Inorg. Chim. Acta* **2013**, *406*, 205−210.

(18) Han, S. J.; Wang, Y.; Pan, S. L.; Dong, X.; Wu, H. P.; Han, J.; Yang, Y.; Yu, H. W.; Bai, C. Y. *Cryst. Growth Des.* **2014**, *14*, 1794−1801.

(19) Dong, X. Y.; Wu, H. P.; Shi, Y. J.; Yu, H. W.; Yang, Z. H.; Zhang, B. B.; Chen, Z. H.; Yang, Y.; Huang, Z. J.; Pan, S. L.; Zhou, Z. X. *Chem.—Eur. J.* **2013**, *19* (23), 7338−7341.

(20) (a) Alekel, T., III; Keszler, D. A. *Inorg. Chem.* **1993**, *32* (1), 101−105. (b) Alekel, T.; Keszler, D. A. *Acta Crystallogr.* **1992**, *C48*, 1382−1386. (c) Reckeweg, O.; Schulzb, A.; DiSalvo, F. J. *Z. Naturforsch.* **2011**, *66b*, 359−365.

(21) (a) Egorova, B. V.; Olenev, A. V.; Berdonosov, P. S.; Kuznetsov, A. N.; Stefanovich, S. Y.; Dolgikh, V. A.; Mahenthirarajah, T.; Lightfoot, P. *J. Solid State Chem.* **2008**, *181* (8), 1891−1898. (b) Plachinda, P. A.; Dolgikh, V. A.; Stefanovich, S. Y.; Berdonosov, P. S. *Solid State Sci.* **2005**, *7*, 1194−1200.

(22) (a) Chen, Z. H.; Pan, S. L.; Yang, Z. H.; Dong, X. Y.; Su, X.; Yang, Y. *J. Mater. Sci.* **2013**, *48*, 2590−2596. (b) Belokoneva, E. L.; Kabalov, Yu. K.; Dimitrova, O. V.; Stefanovich, S. Yu. *Kristallografiya* **2003**, *48*, 44−48.

(23) Dong, L. Y.; Pan, S. L.; Wu, H. P.; Su, X.; Yu, H. W.; Wang, Y.; Chen, Z. H.; Huang, Z. J.; Yang, Z. H. *J. Solid State Chem.* **2013**, *204*, 64−69.

(24) *SAINT*, Version 7.60A; Bruker Analytical X-ray Instruments, Inc.: Madison, WI, 2008.

(25) Sheldrick, G. M. *SHELXTL*, version 6.14; Bruker Analytical X-ray Instruments, Inc.: Madison, WI, 2008.

(26) Spek, A. L. *J. Appl. Crystallogr.* **2003**, *36*, 7−13.

(27) (a) Maggard, P. A.; Nault, T. S.; Stern, C. L.; Poeppelmeier, K. R. *J. Solid State Chem.* **2003**, *175*, 27−33. (b) Choyke, S. J.; Blau, S. M.;

Larner, A. A.; Sarjeant, A. N.; Yeon, J.; Halasyamani, P. S.; Norquist, A. J. *Inorg. Chem.* **2009**, *48*, 11277−11282.
(28) Kurtz, S. K.; Perry, T. T. *J. Appl. Phys.* **1968**, *39*, 3798−3813.
(29) Tauc, J. *Mater. Res. Bull.* **1970**, *5*, 721−730.
(30) (a) Yu, H. W.; Pan, S. L.; Wu, H. P.; Yang, Z. H.; Dong, L. Y.; Su, X.; Zhang, B. B.; Li, H. Y. *Cryst. Growth Des.* **2013**, *13*, 3514−3521. (b) Shi, Y. J.; Pan, S. L.; Dong, X. Y.; Wang, Y.; Zhang, M.; Zhang, F. F.; Zhou, Z. X. *Inorg. Chem.* **2012**, *51*, 10870−10875. (c) Zhou, L.; Pan, S. L.; Dong, X. Y.; Yu, H. W.; Wu, H. P.; Zhang, F. F.; Zhou, Z. X. *CrystEngComm* **2013**, *15*, 3412−3416.
(31) Clark, S. J.; Segall, M. D.; Pickard, C. J.; Hasnip, P. J.; Probert, M. J.; Rrfson, K.; Payne, M. C. Z. *Kristallografiya* **2005**, *220*, 567−570.
(32) Lee, M.-H. Ph.D. Thesis, The University of Cambridge, 1996.
(33) Lin, J.; Qteish, A.; Payne, M.; Heine, V. *Phys. Rev. B* **1993**, *47*, 4174−4180.
(34) Rappe, A. M.; Rabe, K. M.; Kaxiras, E.; Joannopoulos, J. D. *Phys. Rev. B* **1990**, *41*, 1227−1230.
(35) Perdew, J. P.; Burke, K.; Ernzerhof, M. *Phys. Rev. Lett.* **1996**, *77*, 3865−3868.
(36) (a) Grice, J. D.; Burns, P. C.; Hawthorne, F. C. *Can. Mineral.* **1999**, *37*, 731−762. (b) Burns, P. C.; Grice, J. D.; Hawthorne, F. C. *Can. Mineral.* **1995**, *33*, 1131−1151.
(37) Glazer, A. M. *Acta Crystallogr.* **1972**, *B28*, 3384−3392.
(38) Glazer, A. M. *Acta Crystallogr.* **1975**, *A31*, 756−762.
(39) Halasyamani, P. S. *Chem. Mater.* **2004**, *16* (19), 3586−3592.
(40) (a) Zhang, J. J.; Zhang, Z. H.; Zhang, W. G.; Zheng, Q. X.; Sun, Y. X.; Zhang, C. Q.; Tao, X. T. *Chem. Mater.* **2011**, *23* (16), 3752−3761. (b) Welk, M. E.; Norquist, A. J.; Arnold, F. P.; Stern, C. L.; Poeppelmeier, K. R. *Inorg. Chem.* **2002**, *41* (20), 5119−5125. (c) Izumi, H. K.; Kirsch, J. E.; Stern, C. L.; Poeppelmeier, K. R. *Inorg. Chem.* **2005**, *44* (4), 884−895.
(41) (a) Aversa, C.; Sipe, J. *Phys. Rev. B* **1995**, *52*, 14636−14645. (b) Lin, J.; Lee, M. H.; Liu, Z. P.; Chen, C. T.; Pickard, C. J. *Phys. Rev. B* **1999**, *60*, 13380−13389. (c) Rashkeev, S. N.; Lambrecht, W. R. L.; Segall, B. *Phys. Rev. B* **1998**, *57*, 3905−3919.
(42) (a) Zhao, W. W.; Pan, S. L.; Han, J.; Yao, J. Y.; Yang, Y.; Li, J. J.; Zhang, M.; Zhang, L. H.; Hang, Y. *J. Solid State Chem.* **2011**, *184*, 2849−2853. (b) Wang, Y. J.; Pan, S. L.; Tian, X. L.; Zhou, Z. X.; Liu, G.; Wang, J.; Jia, D. Z. *Inorg. Chem.* **2009**, *48*, 7800−7804.